

Phase ordering percolation and domain-wall survival in segregating binary Bose–Einstein condensates

Hiromitsu Takeuchi,* Yumiko Mizuno, and Kentaro Dehara

Department of Physics, Osaka City University, 3-3-138 Sugimoto, Sumiyoshi-ku, Osaka 558-8585, Japan

(Dated: December 3, 2024)

Percolation theory is applied to the phase transition dynamics of domain pattern formation in segregating quasi-two-dimensional binary Bose–Einstein condensates. Our numerical experiments revealed that the percolation threshold is close to 0.5. A long-range open domain wall appears with a fractal dimension between two percolating domains. Such a wall can survive for a long time as a relic of the phase transition according to the dynamic finite-size-scaling hypothesis, which seems to be in contrast to the current understanding in cosmology that an infinite defect violates a scale invariance.

PACS numbers: 67.85.Fg, 64.60.ah 47.37.+q, 98.80.Cq

The phase transition dynamics of spontaneous symmetry breaking (SSB) is an important problem discussed in different fields such as condensed matter physics, cosmology, and high energy physics [1–4]. It is believed that the SSB transition causes the nucleation of topological defects due to the Kibble–Zurek mechanism (KZM) in the early universe [5, 6]. Because it is difficult to examine the KZM in our universe experimentally, the defect-nucleation problem has been attracting much attention in the systems of helium superfluids and atomic Bose–Einstein condensates (BECs), given the analogy in SSB between our universe and the quantum fluids [4, 6–12].

Linear and planar defects such as strings and domain walls form a complicated network in quenched phase transition dynamics. The nucleated defect is destroyed if it is closed; e.g., a closed loop of a quantized vortex (cosmic string) can shrink and finally collapse owing to the interactions with phonons/quasiparticles (gravitational waves) [13–16], except for a specific case known as vortons [1, 7, 17]. An open defect across the system can survive. It is important to study how topological defects survive for a long time after the SSB phase transition begins because the solution to this problem can provide an answer to the interesting question of whether or not topological defects are present in our current universe.

In cosmology, it is suggested that percolation is important for understanding the defect-survival problem [18, 19]. Standard percolation (SP) theory [20] aims to describe the quite common problem of how a connected element “percolates” (penetrates through the system). Critical-scaling behavior appears when the occupation rate p of the element considered approaches a threshold p_c over which there appears a percolating cluster. Regarding a real scalar field as the order parameter due to SSB under consideration, a domain wall is formed along the boundary between two spatial domains with positive and negative values in the field. Therefore, an open

domain wall can appear when positive and negative domains simultaneously percolate with $p_c \leq 0.5$. The study of open domain walls is fundamental to understanding open strings because a string may be considered as the intersection of two open domain walls in the real and imaginary parts of a complex scalar field [20]. These arguments sound quite reasonable, and it is meaningful to tackle the defect-survival problem in such a direction by utilizing the quantum fluid systems.

In this work, we study theoretically the percolation problem of phase transition dynamics in segregating binary BECs. A finite-size-scaling (FSS) analysis of our numerical experiments shows that the percolation threshold in strongly segregated BECs is $p_c \approx 0.5$ independently of the intercomponent interaction. We find that a long-range domain wall can exhibit scaling behavior at $p = 0.5$. According to our dynamic FSS analysis, these results can be applied to the later stages of the phase-ordering development, and a domain wall with a noninteger fractal dimension can then survive for a long time.

We consider binary BECs in a quasi-two-dimensional system without external potentials under periodic boundary conditions. By introducing the order parameter $\psi_j = \sqrt{n_j}e^{i\theta_j}$ ($j = 1, 2$) for the j th component at low temperatures, the system obeys the Gross–Pitaevskii (GP) Lagrangian [21] $\mathcal{L} = \int dx dy [\sum_{j=1,2} (i\hbar\psi_j^* \partial_t \psi_j - \frac{\hbar^2}{2m} |\nabla \psi_j|^2) - V]$ with the potential energy density

$$V = \frac{g(1 + \gamma_{12})}{4}(n_1 + n_2)^2 + \frac{g(1 - \gamma_{12})}{4}(n_1 - n_2)^2, \quad (1)$$

where m is the particle mass, and g and $g\gamma_{12}$ are the intracomponent and intercomponent coupling constants, respectively. The total energy and norm $N_j = \int dx dy n_j$ are conserved quantities during the time development. For $\gamma_{12} > 1$, the second term on the right-hand side of Eq. (2) becomes negative with $n_d \equiv n_1 - n_2 \neq 0$, and binary BECs undergo a spontaneous breaking of the Z_2 symmetry with $n_d = n$ or $n_d = -n$, leading to domain formation [22–25]. The density n_j becomes almost zero in the domains of the $k(\neq j)$ th component. A straight domain

*Electronic address: hirotake@sci.osaka-cu.ac.jp;
URL: <http://hiromitsu-takeuchi.appspot.com/>

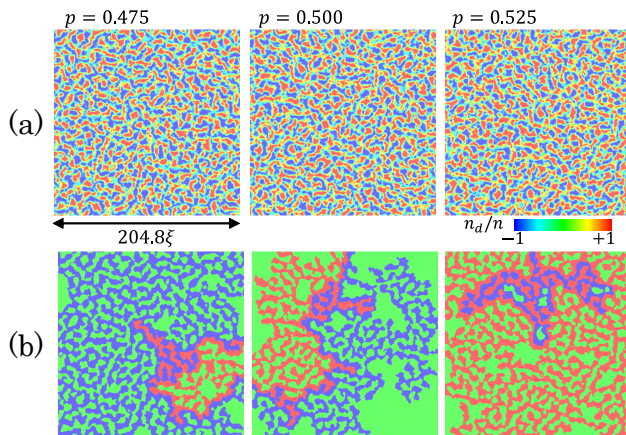


FIG. 1: (Color online) (a) The initial domain patterns of the density difference n_d with $l \approx l_0$ for $\gamma_{12} = 2.0$, $L = 204.8\xi$, and $p = 0.475, 0.500, 0.525$. (b) The maximum domain of (a) is represented by a red (blue) region for the 1st (2nd) component.

wall is stabilized under the pressure balance $P_1 = P_2$ with the hydrostatic pressure $P_j = gn_j^2/2$ in the domain of the j th component. By neglecting the thickness and curvature of the walls, we may write $n_j \approx n \equiv (N_1 + N_2)/2L^2$ at a place far from domain walls. Without loss of generality, we consider the 1st component as the percolation element discussed below; then, the occupation rate is defined as $p = N_1/(N_1 + N_2)$.

Figure 1(a) shows the characteristic domain patterns emerging during the early stages of the time development for different values of p obtained by numerically solving the GP equations derived from the Lagrangian. The initial state for the numerical computation is the fully miscible state with $n_j(t=0) = N_j/L^2$ with a system size L . In our simulation, the dynamic instability is triggered by initially introducing a random fluctuation with a small amplitude δ . For a strong instability, the initial domain pattern emerging in the early stages is characterized by the wave number k_M of the Bogoliubov mode with the maximum imaginary part Γ_M in the dispersion [21].

For the case of $(N_1 - N_2)/N \ll 1$, we have $k_M \sim \sqrt{\gamma_{12} - 1}/\xi$ and $\Gamma_M \sim (\gamma_{12} - 1)/2\tau$ with $\xi = \hbar/\sqrt{gmn}$ and $\tau = \hbar/gn$. Then, the instability is characterized by the length l_0 and time τ_0 as follows:

$$l_0 \equiv \pi(\gamma_{12} - 1)^{-1/2} \xi \quad (2)$$

$$\tau_0 \equiv 2\pi \ln(n/2\delta^2) (\gamma_{12} - 1)^{-1} \tau \quad (3)$$

In fact, we found that the domain patterns become clear around $t = \tau_0$ with the mean interwall distance $l \approx l_0$ [see examples in Fig. 1(a)]. Here, l is computed by numerically integrating the total length $R = L^2/l$ of the domain-wall line, defined by $n_d = 0$ [26]. For $\tau \gtrsim \tau_0$, $l(t)$ obeys a characteristic power law, which is typical behavior in the kink formation dynamics observed in similar

systems [27–30]; however, this is not the main topic of our work.

Here, we mention the main target—open domain walls in the domain patterns. We are interested in long-range open walls, which are distributed across the system. A long-range wall is realized between the two domains, both of which simultaneously span the system in the same direction, i.e., from $x = -\infty$ to $x = \infty$ (or from $y = -\infty$ to $y = \infty$). Such a directed open wall is deformed into a straight wall owing to some dissipative mechanism, which smoothens the domain-wall lines, to survive for long after the phase transition dynamics begin, although closed walls shrink and subsequently vanish [31].

A long-range open wall exists as an interface between the two domains, whose area is the largest in each component. In our dynamical system, evaluation of the survival of open domain walls is not straightforward. A directed open wall can be transformed into a nondirected open wall after a few reconnections of the wall with other short walls. An example of such a nondirected wall is demonstrated in Fig. 1(b) for $p = 0.500$, where the wall runs from $x = -L/2$ to $y = L/2$. Conversely, it is easy to create a directed wall from such a long nondirected wall. Thus, an open wall between the maximum domains has the potential to survive as “a relic” of the transition. We call such a long-range wall the relic wall. We will evaluate the possibility of a relic wall in connection with the statistical properties of the maximum domains. SP theory [20] is useful to the evaluation.

To demonstrate the direct relation of our system with the percolation problem, we computed the ensemble average of the area $S_M(p, L)$ of the maximum domain. According to SP theory [20], the percolation probability in our system may be represented by $\lim_{L \rightarrow \infty} [S_M(p, L)/L^2]$. Then, the percolation problem is analyzed by the quantity

$$P(p, L) \equiv \langle S_M(p, L) \rangle_l / L^2, \quad (4)$$

where $\langle \dots \rangle_l$ represents the ensemble average with l fixed. The average of the domain patterns with $|l(t) - l_0|/l_0 \lesssim 0.005$ was obtained by performing numerical simulations $N_L (\geq 6.553.6 \times \xi/L)$ times. We found that the maximum domain spans the system probably if $p \gtrsim 0.5$ ($p \lesssim 0.5$) for the 1st (2nd) component [see Fig. 1(b)]. Actually, $P(p, L)$ increases rapidly from $p \sim 0.5$. This upturn becomes sharper for a larger system size, and the probability asymptotically approaches $P(p, L) \rightarrow p$ for $p \rightarrow 1$. These behaviors are consistent with the finite-size effect in the SP systems [20].

To confirm the scaling behavior of SP in our system, we perform a FSS analysis [20]. It is convenient to utilize the property of the parameter $P(p, L)L^{\beta/\nu}$ with the critical exponents $\beta = 5/36$ and $\nu = 4/3$ [20]. This parameter takes a universal value independent of the system size L at $p = p_c$:

$$P(p_c, L)L^{\beta/\nu} = \text{const.} \quad (5)$$

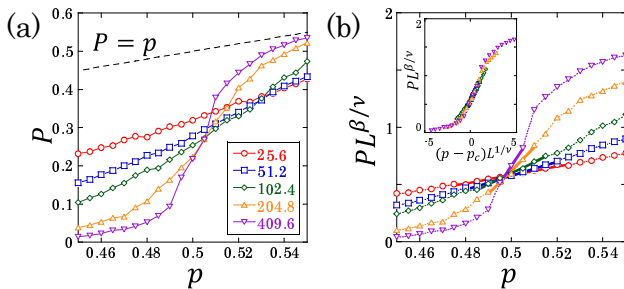


FIG. 2: (Color online) (a) Plots of the probability $P(p, L)$ for $\gamma_{12} = 2.0$ and $L/\xi = 25.6, 51.2, 102.4, 204.8, 409.6$. (b) Plots of the parameter $P(p, L)L^{\beta/\nu}$. The threshold p_c is determined by averaging the positions of all intersection points between the fitting functions represented with bold solid lines. The inset is the finite-size-scaling plot of (a).

This property is used to estimate the percolation threshold [32]. This estimation is sufficient for our main purpose, although the so-called Binder parameter is typically used to determine the critical point of the phase transition [33]. Figure 2 shows the p dependence of $P(p, L)L^{\beta/\nu}$ for several values of L . The plots with different values of L collapse onto a point at $p \sim 0.5$.

The percolation threshold is estimated by fitting a plot with a linear function in the least-squares method for $0.5 - \delta p_L \leq p \leq 0.5 + \delta p_L$ with $\delta p_L = 0.005 \times 409.6 \xi / L$ [see in Fig. 2(b)]. We averaged the positions of all intersection points between the fitting lines with two different values of L and obtained $p_c = 0.497(2)$ for $\gamma_{12} = 2.0$ [34]. According to the FSS hypothesis [20], the quantity $P(p, L)$ is scaled by a scaling function $F(x)$ of $x = L^{1/\nu} \Delta p$ with $\Delta p = p - p_c$ as $P(p, L)L^{\beta/\nu} = F(L^{1/\nu} \Delta p)$. The scaling plot is successful when using the above value of p_c [see inset of Fig. 2(a)]. This result clearly shows that our system actually obeys SP theory.

To gain a deeper insight, it is fruitful to investigate how the percolation behavior depends on the intercomponent interaction, which affects the correlation of the domain patterns. It is known that the percolation threshold is sensitive to the correlation between elements, i.e., the number of vertices in bond percolation and the intersite interaction in annealed percolation [20, 35–37]. The most important report related to our purpose is that the percolation threshold and the probability of the simultaneous percolation of two components can change depending on the correlation in the two-dimensional model of a two-phase flow [38].

In our system, namely, a two-phase superflow, the correlation is controllable via the intercomponent interaction: the coherence (or healing) length $\xi_d \sim \xi / \sqrt{\gamma_{12} - 1}$ of the field n_d . However, we found that the percolation threshold remains $p_c \approx 0.5$ insensitively to γ_{12} ; $p_c = 0.498(4), 0.498(1)$, and $0.496(2)$ for $\gamma_{12} = 1.7, 2.5$, and 3.0 , respectively. The point is that segregated binary BECs are classified into strong segregation ($\gamma_{12} \gtrsim 1.7$)

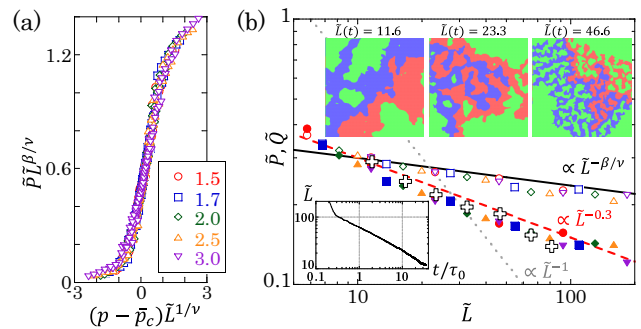


FIG. 3: (Color online) (a) The rescaling plot with the threshold \bar{p}_c . The probability $P(p, L)$ with $L/\xi = 25.6, 51.2, 102.4, 204.8, 409.6$ is rescaled for $\gamma_{12} = 1.5, 1.7, 2.0, 2.5, 3.0$. (b) The \tilde{L} -dependence of the relic probability \tilde{Q} (filled marks). A plot of the rescaled percolation probability \tilde{P} at $p = 0.5$ is displayed with the same marks as in (a). White crosses represent the dynamical plot of $\tilde{Q}(\tilde{L}(t))$ with $\gamma_{12} = 2.0$ and $L/\xi = 204.8$ for several values of $\tilde{L}(t) = L/l(t)$. Insets: a typical time evolution of $\tilde{L}(t)$ (lower left) and snapshots of the maximum domains in a numerical simulation at $t/\tau_0 \approx 2, 9$, and 33 with $\tilde{L} = 46.6, 23.3$, and 11.6 , respectively (upper right).

and weak segregation ($1 < \gamma_{12} \lesssim 1.7$), which are related to the competition between ξ_d and the healing length of the total density $n_1 + n_2$ [39]. Nevertheless, we did not find any qualitative change around $\gamma_{12} = 1.7$.

This fact makes us expect that domain patterns with different γ_{12} can be universally described as having the same statistical property. The FSS analysis is applied after L is scaled by the characteristic domain size, that is the mean interwall distance $l = l_0(\gamma_{12})$. Then, the probability in Eq. (4) is rescaled by the effective system size $\tilde{L} = L/l$ as

$$\tilde{P}(p, \tilde{L}) \tilde{L}^{\beta/\nu} = \tilde{F}(\tilde{L}^{1/\nu} \Delta p), \quad (6)$$

where we used the relation $\tilde{P}(p, \tilde{L}) = P(p, L)$ and the rescaling function \tilde{F} . This conjecture is confirmed by the successful overlapping of the rescaling plots by using the average value of the thresholds of $\gamma_{12} = 1.7, 2.0, 2.5$, and 3.0 , $\bar{p}_c \approx 0.497$, in Fig. 3(a). Our rescaling plot successfully includes the data for $\gamma_{12} = 1.5$ [40]. From this fact, we conclude that the percolation properties of this system are nearly independent of γ_{12} , although we cannot examine the limit $\gamma_{12} \rightarrow 1$ because of the difficulty in numerical simulation with $\tau_0 \rightarrow \infty$ and $l_0 \rightarrow \infty$.

Now, let us return to the relic-wall problem. To evaluate the spatial distribution of the relic wall, we introduce the relic-wall length R_M and the probability that a specific wall segment belongs to the relic wall:

$$Q(L) \equiv \langle R_M / R \rangle_l = l \langle R_M \rangle_l / L^2 \quad (7)$$

We consider the rate $p = 0.5$, with which the dynamical analysis is valid, as discussed later. Because this rate is

very close to the percolation threshold, we assume that the two maximum domains have the scaling behavior described by SP theory. From Eqs. (4) and (5), we have $S_M(p \rightarrow p_c, L) \propto L^{D_S}$, and the percolating domain has the fractal dimension $D_S = 2 - \beta/\nu$. Similarly, we assume the scaling behavior

$$R_M(L) \propto L^{D_R} \quad (8)$$

with the fractal dimension D_R of the relic wall.

The fractal dimensions D_R and D_S are related to each other in the following way. If domain walls are homogeneously distributed throughout the system, the relic probability $Q(L)$ is considered to be the ratio of the area occupied by the relic wall to the system area L^2 . Because the relic wall is sandwiched between percolating domains, the area ratio must be smaller than the right-hand side of Eq. (4), which is the area ratio of the maximum domains to L^2 . Then, for large L , the following condition should be satisfied:

$$1 \leq D_R \leq D_S. \quad (9)$$

The lowest limit originates from the requirement $R_M \gtrsim L$.

A rescaling analysis is convenient to produce a unified description of the scaling behavior of our system. From the fractal behavior of the maximum domain, we have

$$\tilde{P}(p \rightarrow p_c, \tilde{L}) \sim \tilde{L}^{-\beta/\nu}. \quad (10)$$

In the same way, the relic probability $\tilde{Q}(\tilde{L}) = Q(L)$ is written as

$$\tilde{Q}(\tilde{L}) \sim \tilde{L}^{-h} \quad (11)$$

with the exponent $h \equiv 2 - D_R$. Then, the condition (9) reduces to

$$\beta/\nu \leq h \leq 1. \quad (12)$$

Figure 3(b) shows the rescaling plots of $\tilde{Q}(\tilde{L})$ for the initial domain pattern with $\tilde{L} = L/l_0(\gamma_{12})$. The condition (12) is actually satisfied with $h \approx 0.3$. For comparison, we plot $\tilde{P}(p = 0.5, \tilde{L})$, which is consistent with Eq. (10). Our scaling analysis is well applicable for $L \ll l$. This is why \tilde{P} does not obey this law below $\tilde{L} \sim 10$. Our results show that a relic wall has scaling behavior with a noninteger fractal dimension with $D_R \approx 1.7$.

The relic wall will maintain the scaling behavior for a long time during the phase ordering development because the system with $p \sim 0.5$ obeys the dynamic scaling law [30, 41]. The law states that the domain patterns at a later time appear statistically similar to those at an

early time if the patterns are scaled by the characteristic domain size $l(t)$. Then, we may replace $\tilde{L} = L/l_0$ in the above analysis with the dynamical value $\tilde{L}(t) = L/l(t)$.

To test this argument, we computed the relic probability $\tilde{Q}(\tilde{L}(t))$ for $l(t)/l_0 = 0.8, 1.0, 1.4, 2.0, 2.8, 3.9$, and 5.6 by averaging many numerical experiments for $\gamma_{12} = 2.0$ and $L/\xi = 204.8$. We numerically confirmed that the relic wall maintains its scaling behavior with $h \approx 0.3$ during the phase ordering development until a later time with $\tilde{L}(t) \sim 10$.

Experimentally, we will observe a relic domain wall in an atomic cloud whose size is larger than at least dozens of times the length ξ for $\gamma_{12} = 2.0$. Because the dynamic scaling law is applicable to a dissipative system [41], our rescaling analysis can be examined in experiments at a finite temperature if the initial domain patterns are predominantly caused by a dynamic instability. After the mean interwall distance becomes comparable to the size of the atomic clouds, the configuration of the domain walls depends on the details of the system, e.g., the shape of the external potentials.

In conclusion, we found that the percolation threshold of segregating binary BECs is approximately 0.5, and a long-range domain wall with a noninteger fractal dimension can survive for a long time during the phase transition dynamics. It is noteworthy that the domain wall maintains its scaling behavior; in contrast, the system of infinite (open) cosmic strings is believed to not be scale invariant in numerical cosmology [18, 19]. It is also nontrivial that a domain wall exhibits fractal behavior when p_c is not so close to 0.5. Thus, it will be instructive to investigate phase ordering percolation in three dimensions, where the percolation threshold becomes smaller than that in two dimensions in general [19, 20]. Our method and consideration is applicable straightforwardly to three dimensional system. The application of our analysis to different phase ordering systems would also be helpful to verify the exponent h and its relation with other critical exponents.

Acknowledgments

We are grateful to M. Tsukamoto, H. Ishihara, T. Odagaki, M. Takahashi, and M. Kobayashi for useful discussions and comments. This work was partly supported by KAKENHI from JSPS (Grants No. 25887042 and No. 26870500). This work was also partly supported by the Topological Quantum Phenomena (Grants-in-Aid No. 22103003) for Scientific Research on Innovative Areas from the Ministry of Education, Culture, Sports, Science and Technology (MEXT) of Japan.

[1] A. Vilenkin and E. P. S. Shellard, *Cosmic Strings and Other Topological Defects* (Cambridge University Press,

Cambridge, England, 1995).

- [2] A. Onuki, *Phase Transition Dynamics* (Cambridge University Press, Cambridge, England, 2002).
- [3] T. Vachaspati, *Kinks and Domain Walls: An Introduction to Classical and Quantum Solitons* (Cambridge University Press, Cambridge, England, 2006).
- [4] *Topological Defects and the Non-Equilibrium Dynamics of Symmetry Breaking Phase Transitions*, edited by Y. M. Bunkov and H. Godfrin, Vol. 549 of NATO Advance Science Institute, Series C: Mathematical and Physical Sciences (Kluwer, Dordrecht, 2000)
- [5] T. W. B. Kibble, *J. Phys. A* **9**, 1387 (1976).
- [6] W. H. Zurek, *Nature (London)* **317**, 505 (1985); *Phys. Rep.* **276**, 177 (1996).
- [7] G. E. Volovik, *The Universe in a Helium Droplet* (Clarendon, Oxford, 2003).
- [8] P. C. Hendry, N. S. Lawson, R. A. M. Lee, P. V. E. McClintock, and C. D. H. Williams, *Nature (London)* **368**, 315 (1994).
- [9] C. Bäuerle, Yu. M. Bunkov, S. N. Fisher, H. Godfrin, and G. R. Pickett, *Nature (London)* **382**, 332 (1996).
- [10] V. M. H. Ruutu, V. B. Eltsov, A. J. Gill, T. W. B. Kibble, M. Krusius, Yu. G. Makhlin, B. Placais, G. E. Volovik, and W. Xu, *Nature (London)* **382**, 334 (1996).
- [11] L. E. Sadler, J. M. Higbie, S. R. Leslie, M. Vengalattore, and D. M. Stamper-Kurn, *Nature (London)* **443**, 312 (2006).
- [12] C. N. Weiler, T. W. Neely, D. R. Scherer, A. S. Bradley, M. J. Davis, and B. P. Anderson, *Nature (London)* **455**, 948 (2008).
- [13] G. W. Rayfield and F. Reif, *Phys. Rev.* **136**, A1194 (1964).
- [14] N. B. Kopnin and M. M. Salomaa, *Phys. Rev. B* **44**, 9667 (1991).
- [15] V. Berezhinsky, B. Hnatyk, and A. Vilenkin, *Phys. Rev. D* **64**, 043004 (2001).
- [16] T. Damour and A. Vilenkin, *Phys. Rev. Lett.* **85**, 3761 (2000); *Phys. Rev. D* **64**, 064008 (2001); *Phys. Rev. D* **71**, 063510 (2005).
- [17] M. A. Metlitski and A. R. Zhitnitsky, *J. High Energy Phys.* **06**, 017 (2004).
- [18] T. Vachaspati and A. Vilenkin, *Phys. Rev. D* **30**, 2036 (1984).
- [19] T. Vachaspati, in *Topological Defects and the Non-Equilibrium Dynamics of Symmetry Breaking Phase Transitions*, edited by Y. M. Bunkov and H. Godfrin, Vol. 549 of NATO Advance Science Institute, Series C: Mathematical and Physical Sciences (Kluwer, Dordrecht, 2000), p. 55.
- [20] D. Stauffer and A. Aharony, *An Introduction to Percolation Theory*, Revised 2nd. Ed. (Taylor and Francis, London, 1994).
- [21] C. J. Pethick and H. Smith, *Bose-Einstein Condensation in Dilute Gases*, 2nd ed. (Cambridge University Press, Cambridge, 2008).
- [22] S. B. Papp, J. M. Pino, and C. E. Wieman, *Phys. Rev. Lett.* **101**, 040402 (2008).
- [23] R. P. Anderson, C. Ticknor, A. I. Sidorov, and B. V. Hall, *Phys. Rev. A* **80**, 023603 (2009).
- [24] S. Tojo, Y. Taguchi, Y. Masuyama, T. Hayashi, H. Saito, and T. Hirano, *Phys. Rev. A* **82**, 033609 (2010).
- [25] S. De, D. L. Campbell, R. M. Price, A. Putra, B. M. Anderson, and I. B. Spielman, *Phys. Rev. A* **89**, 033631 (2014).
- [26] Exactly speaking, the domain-wall line of $n_d = 0$ is defined as a collection of sides between the computational rectangular meshes with $n_d > 0$ and $n_d < 0$. A saddle point, an intersection of the lines in the mesh space, occasionally occurs when two domain walls are close to each other. We calculated the average value \bar{n}_d of n_d around the saddle point and then regard the point with $\bar{n}_d > 0$ (< 0) as a point occupied by the 1st (2nd) component connecting the diagonal domains with $n_d > 0$ (< 0).
- [27] H. Takeuchi, K. Kasamatsu, M. Tsubota, and M. Nitta, *Phys. Rev. Lett.* **109**, 245301 (2012).
- [28] K. Kudo and Y. Kawaguchi, *Phys. Rev. A* **88**, 013630 (2013).
- [29] M. Karl, B. Nowak, and T. Gasenzer, *Phys. Rev. A* **88**, 063615 (2013).
- [30] J. Hofmann, S. S. Natu, and S. Das Sarma, *Phys. Rev. Lett.* **113**, 095702 (2014).
- [31] A closed wall can be stabilized around a so-called coreless vortex, in which a component is trapped by the core of a quantized vortex in the other component. The core size of such vortices is on the order of the thickness of a domain wall, and we found that not so many vortices appear in our system. Thus, the effect is not important to our analysis.
- [32] A. K. Chandra, *Phys. Rev. E* **85**, 021149 (2012).
- [33] K. Binder, *Z. Phys. B* **44**, 119 (1981).
- [34] There are intrinsically large fluctuations around the threshold $p_c \approx 0.5$. Thus, to achieve the threshold value with satisfactory accuracy, we carried out many more simulations for $0.5 - \delta p_L \leq p \leq 0.5 + \delta p_L$. We computed more than $N_L \times 4$ times for $0.485 \leq p \leq 0.515$ and $N_L \times 8$ times for $p = 0.5$.
- [35] L. J. Duckers and R. G. Ross, *Phys. Lett. A* **49**, 361 (1974); *ibid.* **67**, 93 (1978).
- [36] T. Odagaki, *Prog. Theor. Phys.* **54**, 1067 (1975).
- [37] D. A. Wollman, M. A. Dubson, and Q. Zhu, *Phys. Rev. B* **48**, 3713 (1993).
- [38] D. D. Nolte and L. J. Pyrak-Nolte, *Phys. Rev. E* **56**, 5009 (1997).
- [39] P. Ao and S. T. Chui, *Phys. Rev. A* **58**, 4836 (1998).
- [40] Our numerical experiments become more difficult to perform with decreasing γ_{12} because the computation time and the required system size are proportional to τ_0 and l_0 , respectively. For this reason, we could not determine the threshold for $\gamma_{12} = 1.5$ with satisfactory accuracy.
- [41] A. J. Bray, *Adv. Phys.* **43**, 357 (1994).